JACS
JOURNAL OF THE AMERICAN CHEMICAL SOCIETY
Communication
pubs.acs.org/JACS

Nanostructured Polyaniline-Decorated Pt/C@PANI Core–Shell Catalyst with Enhanced Durability and Activity

Siguo Chen,[†] Zidong Wei,*[,†] XueQiang Qi,[†] Lichun Dong,[†] Yu-Guo Guo,[‡] Lijun Wan,*[,‡] Zhigang Shao,[§] and Li Li[†]

[†]State Key Laboratory of Power Transmission Equipment & System Security and New Technology, College of Chemistry and Chemical Engineering, Chongqing University, Chongqing 400044, China

[‡]Key Laboratory of Molecular Nanostructure and Nanotechnology, Institute of Chemistry, Chinese Academy of Sciences, Beijing 100190, China

[§]Dalian Institute of Chemical Physics, Chinese Academy of Sciences, Dalian Liaoning 116023, China

Supporting Information

ABSTRACT: We have designed and synthesized a polyaniline (PANI)-decorated Pt/C@PANI core–shell catalyst that shows enhanced catalyst activity and durability compared with nondecorated Pt/C. The experimental results demonstrate that the activity for the oxygen reduction reaction strongly depends on the thickness of the PANI shell and that the greatest enhancement in catalytic properties occurs at a thickness of 5 nm, followed by 2.5, 0, and 14 nm. Pt/C@PANI also demonstrates significantly improved stability compared with that of the unmodified Pt/C catalyst. The high activity and stability of the Pt/C@PANI catalyst is ascribed to its novel PANI-decorated core–shell structure, which induces both electron delocalization between the Pt d orbitals and the PANI π-conjugated ligand and electron transfer from Pt to PANI. The stable PANI shell also protects the carbon support from direct exposure to the corrosive environment.

Proton exchange membrane fuel cells (PEMFCs) are regarded as ideal candidates for stationary and mobile power generation because of their high energy conversion efficiencies and low environmental impact.[1] However, the insufficient electrocatalytic activity and durability of Pt cathode catalysts still remains a major obstacle for PEMFC applications.[2] At present, the most commonly used cathode catalysts are highly dispersed 2–5 nm Pt nanoparticles (NPs) supported on carbon. However, Pt NPs suffer from poor durability because of the rapid and significant loss of platinum electrochemical surface area (ECSA) over time due to corrosion of the carbon support, Pt dissolution, Ostwald ripening, and aggregation.[3]

Aside from durability issues, the high cost of Pt cathode catalysts is another obstacle that has hindered the development of PEMFCs because of the world's limited Pt reserves. Therefore, many recent studies have focused on decreasing the Pt loading and increasing the Pt utilization while maintaining satisfactory activity and stability; such efforts include the design of new catalyst structures,[4] alloying of Pt with other transition metals,[5] the development of new durable catalyst supports,[6] modification of Pt NPs with other species,[3a] and optimization of the catalyst structure to increase the exposure of Pt NPs to the three-phase zone.[7] Although these methods have been proposed to enhance the catalytic activity and durability, the development of a Pt-based catalyst with both good durability and high mass activity remains a challenge.

Conducting polymers such as polypyrrole (PPy) and polyaniline (PANI) have received special attention in fuel cell applications because of their unique π-conjugated structures, which lead to good environmental stability, high electrical and proton conductivity in acidic environments, and unique redox properties.[8] Recently, Deki and co-workers[9] reported the preparation of a Pt/electroconductive-polymer-loaded carbon composite that improved the durability of electrodes in fuel cells. In that study, $Pt(NH_3)_4^{2+}$ was absorbed onto carbon and used to oxidize aniline while reducing the $Pt(NH_3)_4^{2+}$ itself. The Pt and PANI were thoroughly mixed together throughout the entire polymerization process. Accordingly, nearly all of the Pt NPs in the prepared Pt/PANI/C composite, except those present on the outermost catalyst layer, were embedded inside the PANI rather than exposed to the outside. Thus, some of the Pt NPs could not be utilized by the fuel cell, and the Pt/PANI/C composites showed poor oxygen reduction reaction (ORR) activity; indeed, no Pt behavior was observed in cyclic voltammograms (CVs) of the Pt/PANI/C composites. Although Pt/PANI/C composites showed better durability than Pt/C catalysts, they are unsuitable for fuel cell applications, where the Pt NPs must be exposed to the three-phase zone.

Herein we discuss the design and synthesis of a Pt/C@PANI core–shell-structured catalyst that addresses both the activity and durability issues. The catalyst was prepared through the direct polymerization of a thin layer of PANI on the carbon surface of the Pt/C catalyst. In the present work, as shown in Scheme 1, the aniline monomer was first selectively adsorbed onto the carbon surface via preferential π–π conjugation between the aniline and the carbon support and was then polymerized in situ on the carbon surface via ammonium peroxodisulfate (APS) oxidation in acidic solution [see the

Received: July 4, 2012
Published: August 1, 2012

dx.doi.org/10.1021/ja306501x | J. Am. Chem. Soc. 2012, 134, 13252–13255

Scheme 1. Configuration of the Pt/C@PANI Catalyst

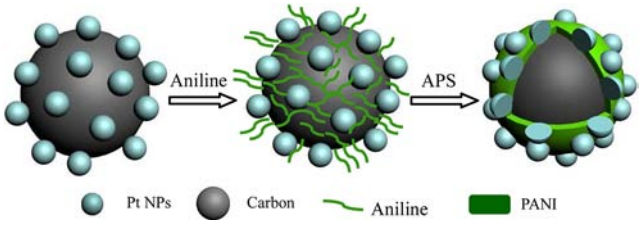

Supporting Information (SI)]. Unlike the Pt/PANI/C composite, in which most of the Pt NPs are wrapped in PANI and cannot be utilized by the fuel cell reaction,[9] the PANI shell layer in the Pt/C@PANI core–shell catalyst preferentially and selectively covers the surface of the carbon rather than that of the Pt. Electrochemical measurements confirmed that this unique catalyst structure has excellent ORR activity and electrochemical durability and that the activity highly depends on the thickness of the PANI shell; the greatest enhancement in the catalytic properties occurred at a thickness of 5 nm, followed by 2.5, 0, and 14 nm.

Figure 1 presents typical high-resolution transmission electron microscopy (HRTEM) images of Pt/C@PANI

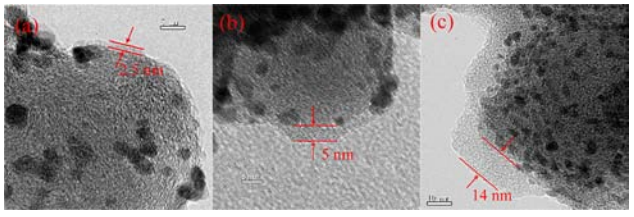

Figure 1. HRTEM images of the Pt/C@PANI catalysts with PANI loadings of (a) 20, (b) 30, and (c) 50%.

catalysts with different PANI contents, which clearly exhibit the core–shell structure illustrated in Scheme 1. The cores of the Pt/C catalyst particles were well covered with a PANI shell layer. The average thicknesses of the PANI shells were ~2.5, ~5, and ~14 nm for Pt/C@PANI specimens with PANI loadings of 20, 30, and 50%, respectively, which suggests that the thickness of the PANI shell can be controlled via the PANI loading. The Fourier transform IR spectroscopy (FTIR) spectrum of the Pt/C@PANI specimen (Figure S1 in the SI) confirmed chemical identity of the outer-shell coating to be PANI. Prior to the application of the PANI coating, a strong peak detected at 1610 cm^{-1} for the Pt/C catalyst was attributed to the carbonyl groups of the carbon support material.[10] After the deposition of the PANI shell, the characteristic carbonyl peak disappeared and was replaced by five major bands at 823, 1135, 1310, 1500 and 1590 cm^{-1}; these peaks are associated with PANI,[11] suggesting that the surface of the carbon support was sufficiently covered with PANI. The difference in the FTIR spectra of Pt/C@PANI (30%) and pure PANI is the shift in the characteristic bands to relatively higher wavenumbers in the spectrum of the PANI-coated sample, which suggests the presence of strong interactions between the PANI shell and the carbon support.

The influence of the shell thickness on the electrochemical performance of the Pt/C@PANI catalysts is presented in Figure 2. Figure 2a shows CVs of the Pt/C@PANI catalysts with different PANI contents in a N_2-purged 0.5 M H_2SO_4 solution at a scan rate of 50 mV s^{-1}. The ECSA was calculated

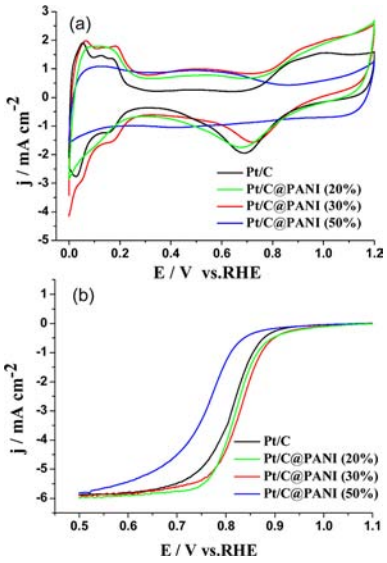

Figure 2. (a) CVs of 40 wt % Pt/C catalyst electrodes made from Pt/C@PANI with different PANI contents in a N_2-purged 0.5 M H_2SO_4 solution at a scan rate of 50 mV s^{-1}. (b) ORR curves of electrodes made from Pt/C and from Pt/C@PANI with different PANI contents in an O_2-saturated 0.5 M H_2SO_4 solution at room temperature (1600 rpm, sweep rate 2 mV s^{-1}).

by measuring the Coulombic charge for hydrogen adsorption. The specific values of the ECSA based on the Pt mass for Pt/C, Pt/C@PANI (20%), Pt/C@PANI (30%), and Pt/C@PANI (50%) were estimated to be 71.4, 67.5, 60.7, and 6.5 m^2 g^{-1}, respectively. The trend of decreasing Pt ECSA with increasing PANI loading suggested that the Pt/C@PANI should not be functional when excessive PANI is loaded onto the catalyst because of the limited penetrability of liquid H_2SO_4 solution in PANI. A high PANI loading could also incorporate the Pt NPs into the polymer network.

The activities of the Pt/C@PANI catalysts with different PANI loadings were measured using a rotating-disk electrode (RDE) operated at 1600 rpm in O_2-saturated 0.5 M H_2SO_4. The polarization curves for the catalysts are shown in Figure 2b. The electrocatalytic activities of the different catalysts, as estimated from the half-wave potentials ($E_{1/2}$),[12] were maximized for Pt/C@PANI (30%) and decreased successively for Pt/C@PANI (20%), Pt/C, and Pt/C@PANI (50%), with $E_{1/2}$ values of 829, 819, 812, and 761 mV vs reversible hydrogen electrode (RHE), respectively. For a better understanding of the ORR activities of the different catalysts, the kinetic current (j_k) associated with the intrinsic activity of each catalyst was obtained by constructing Koutecky–Levich plots for oxygen reduction with the different catalysts (experimental details are provided in the SI).[13] At 0.85 V vs RHE, the mass activities for Pt/C@PANI (30%), Pt/C@PANI (20%), Pt/C, and Pt/C@PANI (50%) were estimated to be 68, 47, 36, and 9 mA mg_{Pt}^{-1}, respectively (Figure S2). Considered together with the observed $E_{1/2}$ values, these data show that the Pt/C@PANI (30%) and Pt/C@PANI (20%) catalysts drastically outperformed the Pt/C@PANI (50%) and Pt/C catalysts. The enhanced catalytic activity may be correlated with the weak adsorption of oxygenate species (e.g., O_{ad} and OH_{ad}) on the Pt surfaces. Figure 2a shows that the current peak associated with the reduction of platinum oxide in the CV obtained on the Pt/C@PANI (30%) shifts toward positive potential by more than 40 mV relative to the Pt/C catalyst. This shift indicates that the

dx.doi.org/10.1021/ja306501x | J. Am. Chem. Soc. 2012, 134, 13252–13255

desorption of the oxygenate species on the Pt/C@PANI (30%) surface is easier than on the Pt/C catalyst. The weak adsorption of oxygenated species onto a Pt surface has been shown to increase its catalytic activity toward the ORR.[14]

The stabilities of the Pt/C@PANI (30%) and Pt/C catalysts were investigated using accelerated stress tests (ASTs), which were performed at room temperature in N_2-saturated 0.5 M H_2SO_4 solutions through the application of cyclic potential sweeps between 0 and 1.2 V vs RHE at a scan rate of 50 mV s^{-1}. The Pt ECSA values for the Pt/C@PANI (30%) and Pt/C catalysts after potential cycling were calculated from their CVs (Figure S3a,b), and the normalized ECSA was plotted as a function of the cycle number (Figure 3a). The Pt ECSA of the

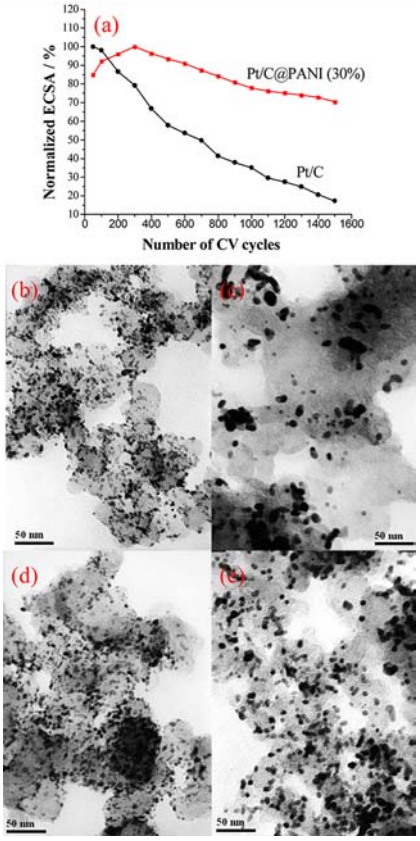

Figure 3. (a) Normalized Pt ECSAs of the electrodes made with Pt/C and Pt/C@PANI (30%) catalysts as functions of the number of CV cycles in N_2-purged 0.5 M H_2SO_4 at room temperature (0−1.2 V vs RHE, sweep rate 50 mV s^{-1}). (b−e) TEM images of (b) the uncycled Pt/C catalyst, (c) the Pt/C catalyst after 1500 CV cycles, (d) the uncycled Pt/C@PANI (30%) catalyst, and (e) the Pt/C@PANI (30%) catalyst after 1500 CV cycles.

Pt/C@PANI (30%) catalyst decreased by only ~30% after 1500 CV cycles, whereas the Pt/C catalyst lost ~83% of its initial ECSA. The morphologies of the Pt/C@PANI (30%) and Pt/C catalysts before and after the CV cycling were examined by TEM (Figure 3b−e). The size distribution of the Pt NPs calculated according to Figure 3 is shown in Figure S4. After the CV cycling, the size of the Pt NPs in the Pt/C catalyst increased from 2−6 to 4−28 nm with a broad size distribution (Figure S4a,b), indicating that ripening or aggregation of the Pt NPs occurred during the CV cycling. In contrast, the size of the Pt NPs in the Pt/C@PANI (30%) catalyst increased only from 2−6 to 3−10 nm (Figure S4c,d), confirming that the Pt/C@PANI (30%) catalyst is more electrochemically stable than the Pt/C catalyst.

The long-term durability of the PANI@Pt/C (30%) and Pt/C catalysts was also examined in a single cell using an AST protocol (see the SI).[15] The polarization curves obtained after every 1000 cycles of the AST protocol with single cells incorporating the PANI@Pt/C (30%) and Pt/C cathode catalysts are shown in Figure 4. The initial performance of

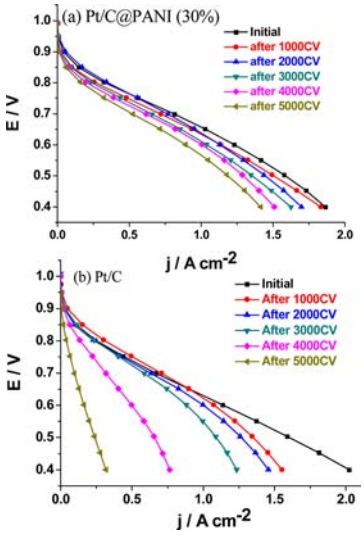

Figure 4. Polarization curves of single PEM fuel cells with cathodes fabricated from (a) PANI@Pt/C (30%) and (b) Pt/C catalysts after the indicated numbers of CV cycles. The Pt loading was 0.3 mg cm^{-2} on the anode and 0.2 mg cm^{-2} on the cathode.

the cell in which the Pt/C catalyst was used was similar to that of the cell in which the PANI@Pt/C (30%) catalyst was used. However, after the AST test was performed, the performance of the cell with the PANI@Pt/C (30%) cathode catalyst showed significantly better durability than the cell with the Pt/C cathode catalyst. For example, the current of the PANI@Pt/C (30%) catalyst cell at 0.6 V decreased from 1.17 to 0.89 A cm^{-2}, whereas the current of the Pt/C catalyst cell decreased from 1.14 to only 0.16 A cm^{-2}. The enhanced stability bestowed by PANI to the PANI@Pt/C (30%) catalysts is unquestionable.

The enhancing effect of PANI on the ORR activity and stability is an interesting phenomenon that is worthy of further investigation. X-ray photoelectron spectroscopy (XPS) of the Pt 4f peak (Figure 5) showed that the Pt $4f_{7/2}$ peak of the Pt/C@PANI (30%) catalyst was shifted to a higher binding energy (72.05 eV) relative to the Pt $4f_{7/2}$ peak of the Pt/C catalyst

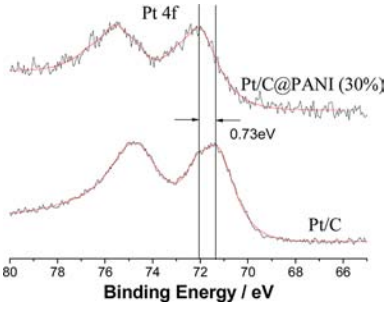

Figure 5. Pt 4f XPS spectra of the Pt/C and Pt/C@PANI (30%) catalysts.

dx.doi.org/10.1021/ja306501x | J. Am. Chem. Soc. 2012, 134, 13252−13255

(71.32 eV). This shift in binding energy is attributed to the electron delocalization between the Pt d orbitals and the PANI π-conjugated ligand and to partial ionization due to electron transfer from Pt to PANI. The electron delocalization between the Pt NPs and PANI alters the electronic structure of the Pt NPs, making it difficult for the Pt NPs to lose/release additional electrons (i.e., to be oxidized). Prevention of the dissolution of Pt via the formation Pt−O bonds is beneficial,[3a,c] and this assertion can be further discerned in the CVs of the Pt/C@PANI (30%) and Pt/C catalysts shown in Figure 2a. The surface oxidation onset potential of the Pt NPs in the Pt/C@PANI (30%) catalyst is more positive than that for the Pt/C catalyst, which indicates that the oxidation of the Pt NPs of Pt/C@PANI (30%) is more difficult.

Quantitative analysis of the XPS spectrum also provided compelling evidence that the PANI shell ameliorated corrosion of the carbon support. Figure S5 shows the XPS spectra of the Pt/C@PANI (30%) and Pt/C catalysts before and after 1500 CV cycles in 0.5 M H_2SO_4 solution. The corresponding results are listed in Table 1. For the Pt/C catalyst, a significant decrease in the amount of surface carbon and an increase in the Pt content was observed after the CV cycling. The loss of carbon from the Pt/C catalyst is attributed to the oxidation of carbon to CO or CO_2. This result further confirms that the electrochemical corrosion of the carbon support is one of the most critical issues affecting the long-term stability of the Pt/C catalyst. In contrast to the dramatic loss of carbon content in the Pt/C catalyst, the Pt/C@PANI (30%) catalyst showed a significant increase in the surface carbon content, demonstrating that corrosion of the carbon support in the Pt/C@PANI (30%) catalyst was prevented to a significant extent by protecting it from direct exposure to the fuel cell reaction interface.

Table 1. Comparison of the Surface Elemental Compositions of the Pt/C and Pt/C@PANI (30%) Catalysts before and after 1500 CV Cycles[a]

sample	C	O	Pt	N	S
Pt/C initial	88.31	10.04	1.66		
Pt/C after cycling	80.80	9.63	9.51		
Pt/C@PANI initial	67.79	22.18	0.36	4.41	5.07
Pt/C@PANI after cycling	76.41	14.29	3.55	4.14	1.61

[a]All values in units of atom %.

In conclusion, we have successfully used in situ chemical oxidation polymerization to prepare a novel Pt/C@PANI core−shell catalyst in which the carbon support is decorated by a PANI layer and the Pt NPs are well-anchored to the carbon surface. The experimental results demonstrate that the ORR activity strongly depends on the thickness of the PANI shell, reaching a maximum at a thickness of 5 nm, followed by 2.5, 0, and 14 nm. Significantly improved stability of the Pt/C@PANI catalyst compared with the unmodified Pt/C catalyst was also observed. The improved activity and stability are attributed to the novel PANI-coated core−shell structure, which results in electron delocalization between the Pt d orbitals and the PANI π-conjugated ligand and in electron transfer from Pt to PANI. The stable PANI shell protects the carbon support from direct exposure to the corrosive environment. These results are significant with respect to the synthesis of highly stable Pt/C catalysts and the enhancement of ORR activity for fuel cell applications.

■ ASSOCIATED CONTENT

Supporting Information

Synthesis conditions; experimental procedures; IR, TEM, and XPS analyses of the catalyst; and ORR activities and CVs of Pt/C and Pt/C@PANI. This material is available free of charge via the Internet at http://pubs.acs.org.

■ AUTHOR INFORMATION

Corresponding Author

zdwei@cqu.edu.cn; wanlijun@iccas.ac.cn

Notes

The authors declare no competing financial interest.

■ ACKNOWLEDGMENTS

This work was financially supported by the China National 973 Program (2012CB215500 and 2012CB720300), the NSFC (Grants 20936008 and 21176327), the Science Research Foundation of SKL-PES (2007DA10512711211), and the Science Research Foundation of Beijing National Laboratory of Molecular Sciences (BNLMS).

■ REFERENCES

(1) Gasteiger, H. A.; Kocha, S. S.; Sompalli, B.; Wagner, F. T. *Appl. Catal., B* **2005**, *56*, 9.

(2) Ferreira, P. J.; la O', G. J.; Horn, Y. S.; Morgan, D.; Makharia, R.; Kocha, S.; Gasteiger, H. A. *J. Electrochem. Soc.* **2005**, *152*, A2256.

(3) (a) Zhang, J.; Sasaki, K.; Sutter, E.; Adzic, R. R. *Science* **2007**, *315*, 220. (b) Yu, X. W.; Ye, S. Y. *J. Power Sources* **2007**, *172*, 145. (c) Shao, Y. Y.; Yin, G. P.; Gao, Y. Z. *J. Power Sources* **2007**, *171*, 558. (d) Chen, Z. W.; Waje, M.; Li, W. Z.; Yan, Y. S. *Angew. Chem., Int. Ed.* **2007**, *46*, 4060.

(4) (a) Wang, J. X.; Mao, C.; Choi, Y. M.; Su, D.; Zhu, Y. M.; Liu, P.; Si, R.; Vukmirovic, M. B.; Zhang, Y.; Adzic, R. R. *J. Am. Chem. Soc.* **2011**, *133*, 13551. (b) Wang, D. L.; Xin, H. L.; Yu, Y. C.; Wang, H. S.; Rus, E.; Muller, D. A.; Abruna, H. D. *J. Am. Chem. Soc.* **2010**, *132*, 17664.

(5) Wang, J. X.; Inada, H.; Wu, L. J.; Zhu, Y. M.; Choi, Y. M.; Liu, P.; Zhou, W. P.; Adzic, R. R. *J. Am. Chem. Soc.* **2009**, *131*, 17298.

(6) Huang, S. Y.; Ganesan, P.; Park, S.; Popov, B. N. *J. Am. Chem. Soc.* **2009**, *131*, 13898.

(7) Chen, S. G.; Wei, Z. D.; Li, H.; Li, L. *Chem. Commun.* **2010**, *46*, 8782.

(8) (a) Coutanceau, C.; Croissant, M. J.; Napporn, T.; Lamy, C. *Electrochim. Acta* **2000**, *46*, 579. (b) Huang, J. X.; Virji, S.; Weiller, B. H.; Kaner, R. B. *J. Am. Chem. Soc.* **2003**, *125*, 314.

(9) (a) Mizuhata, M.; Oga, M.; Deki, S. *ECS Trans.* **2007**, *2* (8), 63. (b) Mizuhata, M.; Oga, M.; Miyachi, Y.; Deki, S. *ECS Trans.* **2008**, *6* (25), 75.

(10) Shao, Y. Y.; Yin, G. P.; Wang, J. J.; Gao, Y. Z.; Shi, P. F. *J. Electrochem. Soc.* **2006**, *153*, A1093.

(11) Ryu, J. K.; Park, C. B. *Angew. Chem., Int. Ed.* **2009**, *48*, 4820.

(12) Zhang, S.; Shao, Y. Y.; Yin, G. P.; Lin, Y. H. *Angew. Chem., Int. Ed.* **2010**, *49*, 2211.

(13) Bard, A. J.; Faulkner, L. R. *Electrochemical Methods: Fundamentals and Applications*; Wiley: New York, 2000.

(14) (a) Stamenkovic, V. R.; Fowler, B.; Mun, B. S.; Wang, G. F.; Ross, P. N.; Lucas, C. A.; Markovic, N. M. *Science* **2007**, *315*, 493. (b) Shao, M. H.; Sasaki, K.; Adzic, R. R. *J. Am. Chem. Soc.* **2006**, *128*, 3526. (c) Kitchin, J. R.; Nørskov, J. K.; Barteau, M. A.; Chen, J. G. *Phys. Rev. Lett.* **2004**, *93*, No. 156801.

(15) Liu, X.; Chen, J.; Liu, G.; Zhang, L.; Zhang, H. M.; Yi, B. L. *J. Power Sources* **2010**, *195*, 4098.